AUTHOR and OTHER-AUTHOR

[Left hand page running head is author's name in Times New Roman 8 point bold capitals, centred. For more than two authors, write **AUTHOR et al.**]

CONFERENCE PRE-PRINT

CHARACTERISTICS OF TUNSTEN SOURCES AND TRANSPORT IN KSTAR PLASMAS

J. JANG, H.H. Lee, D. Seo, C.R. Seon, S. Oh, E.N. Bang Korea Institute of Fusion Energy Daejeon, Republic of Korea Email: jjh4368@kfe.re.kr

A. Grosjean

Department of Nuclear Engineering, University of Tennessee-Knoxville, Tennessee, USA

J.H. Hwang, J.H. Yoon, C. Shin Korea Adavanced Institute of Science and Technology Daejoen, Republic of Korea

Abstract

Following the tungsten divertor installation in KSTAR in 2023, dedicated experiments were conducted to investigate impurity sources and transport. The visible and ultraviolet spectroscopic diagnostics were also upgraded to measure tungsten line emissions from plasma core, edge and divertor regions. In both lower single null and upper single null configuration, the experimental results suggest that the distance between plasma and tungsten divertor strongly influences the tungsten source generation. In addition, RMP-induced ELM mitigation can further suppress impurity generation and accumulation in the core. These findings demonstrate that plasma shaping and RMPs offer effective means for tungsten impurity control.

1. INTRODUCTION

Tungsten (W) is a material of plasma facing components (PFCs) in future fusion devices such as ITER. Since high-Z impurity like tungsten causes significant radiative loss and plasma performance degradation, understanding their behaviour within plasma is essential for tokamak operation. To address these critical physics issues, the KSTAR divertor was upgraded with a tungsten monoblock cassette in 2023, and the first experimental campaign with tungsten divertor has been successfully completed. Initial results revealed that the core plasma radiation is predominantly driven by tungsten impurities transported from the divertor target. dominated by the tungsten impurity transported from the tungsten divertor target. After tungsten divertor installation, both the radiative loss fraction and the average Z_{eff} increased significantly [1, 2].

Further investigation of tungsten impurity behavior and its impact on plasma performance is therefore required. A primary concern is quantifying the amount of tungsten released from the new divertor under various plasma conditions. Building a comprehensive database of tungsten source strengths for different plasma configurations will be valuable for reliable tokamak operation. Another key question is how long tungsten impurities persist in L-mode and H-mode discharges in KSTAR. Since edge-localized modes (ELMs) are known to be a dominant source of tungsten through sputtering of plasma-facing components, impurity production and transport must be systematically studied with and without the presence of ELMs.

This study aims to quantify tungsten sources under a range of plasma positions, shapes, and heating powers, and to investigate the subsequent impurity transport into the core plasma. To investigate W source level with different plasma-target distance, the lower X-point in lower (LSN) and upper single null configurations (USN) were shifted vertically. The effects of resonant magnetic perturbations (RMPs) on tungsten source generation and transport will also be studied. This paper is organized as follows: first, we describe the diagnostic setup for impurity transport studies; preliminary results on tungsten transport under plasma position changes and three-dimensional magnetic fields are then presented; finally, we outline the plans for detailed future analyses.

1

2. EXPERIMENTL SETUP

Following the installation of the tungsten divertor in KSTAR in 2023, the KSTAR visible diagnostic systems [3] were also upgraded. Fig. 1 presents the lines of sight of the optical diagnostics employed in this study. As shown in Fig. 1(a), the toroidal H α monitor consists of 20 channels viewing from the J-port toward the L-port, while the toroidal visible bremsstrahlung (VB) system also comprises 20 channels directed from the J-port toward the H-port. Fig. 1(b) illustrates the poloidal visible channels, where the H α and VB systems share common lines of sight. The spot size and the channel spacing are 2 cm and 5 cm, respectively. During the 2024 campaign, the sampling rate of both the H α and VB systems was 20 kHz. To assess the overall impurity content in the plasma, the Z_{eff} profile are reconstructed from toroidal VB measurements [4].

Several channels of visible survey spectrometers (VSSs) were used to measure line emissions from light impurities at both the plasma center and edge. As shown in Fig. 1(a), one Avantes spectrometer channel is located at the same position as toroidal H α channel 13. The OceanFX (OFX) spectrometers (channels 1–4) observe the lower divertor, upper divertor, plasma center, and outboard edge, respectively. The temporal resolutions of the Avantes and OFX systems are 10 ms and 1 ms, with spectral resolutions of 0.33 nm and 0.1 nm, respectively. The Princeton Instruments (PI) spectrometer was not operated during the 2024 campaign. In addition, a dedicated spectrometer channel was configured for the S/XB method [5], aiming quantification of tungsten influx from the divertor target plates. For W-line detection, the temporal resolution of the S/XB spectrometer was limited to 50 Hz to maximize exposure time, and the spectral resolution was 0.1 nm.

To monitor intrinsic impurity sources during the 2024 campaign, several filterscope channels were equipped with custom bandpass filters. Fig. 1(c) shows the corresponding lines of sight. In the lower divertor, poloidal VB channel #60 and poloidal H α channel #57 were configured to monitor the neutral tungsten (W I, 400.9 nm) line intensity at the central and inner divertor target plates. A bandpass filter for the carbon line (C III,

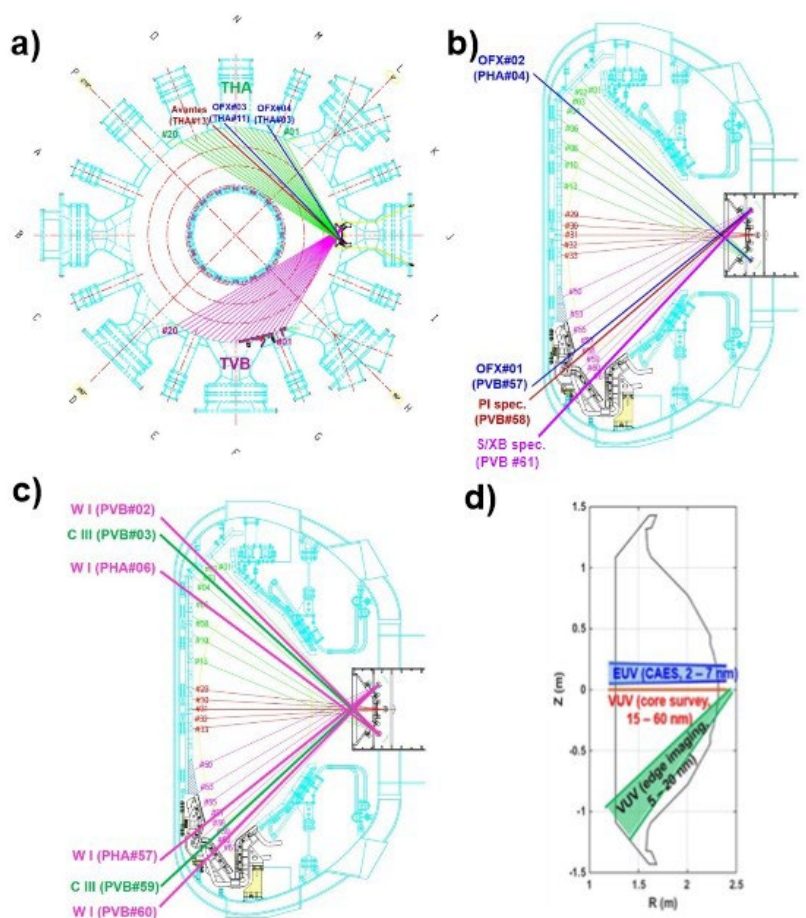


Fig. 1. The lines of sight of **a**) toroidal and **b**) poloidal visible diagnostic system in 2024 KSTAR campaign. **c**) poloidal channels with bandpass filter for impurity monitoring. **d**) The lines of sight of core EUV (CAES), core and edge VUV spectrometer in KSTAR

AUTHOR and OTHER-AUTHOR

[Left hand page running head is author's name in Times New Roman 8 point bold capitals, centred. For more than two authors, write AUTHOR et al.]

464.7 nm) was installed on poloidal VB channel #59. The W I and C III filters had center wavelengths of 400.9 nm and 464.7 nm, respectively, with bandwidths of 1.0 nm. For impurity filterscope analysis, background values were determined by averaging the signal prior to plasma initiation (–0.5 to 0.0 s).

Since tungsten is highly ionized within the confined plasma region, quasi-continuum line emission from highly charged W ions is typically measured by VUV or EUV spectrometers [6, 7]. Fig. 1(d) shows the lines of sight of the KSTAR EUV and VUV systems. The CAES EUV system covers a wavelength range of 1.8–8.3 nm, while the core VUV survey channel covers 12–51.0 nm, with temporal resolutions of 100 ms and 40.8 ms, respectively. In this study, only the core VUV survey signal was used due to its superior time resolution. The divertor VUV imaging system was under maintenance during the 2024 campaign.

3. RESULTS

In 2024, dedicated experiments on tungsten transport were carried out in KSTAR. The primary objectives were to quantify tungsten source levels and to investigate how tungsten transport is modified under various plasma conditions. The reference discharge operated at a plasma current of 0.5 MA, with a maximum heating power of 6.5 MW and a toroidal magnetic field of 1.9 T. In this paper, preliminary results with plasma position change and RMP are presented.

3.1. Tungsten source change with plasma-target distance

The tungsten source level was found to vary with the distance between the plasma and the tungsten divertor target. Fig. 2 shows the time evolution of plasma parameters of discharge #35360. As shown in the left column of Fig. 2(a), global plasma parameters—including electron density, temperature, normalized β , and total radiated power—remained nearly unchanged throughout the discharge. The height of the lower X-point was adjusted to control the plasma—target distance. At the reference position, the lower X-point was located at $(R_X$, $Z_X) = (1.45 \text{ m}, -0.98 \text{ m})$. As shown in the right side top plot in Fig. 2a), at 6.0 s, the X-point was shifted upward by +3.0 cm, then returned to its original position at 9.0 s. At 12.0 s, the X-point was shifted downward by -3.0 cm, with each phase maintained for ~2 s to achieve steady-state tungsten transport conditions.

As seen in Fig. 2(a), plasma parameters remained largely unchanged across phases, and the poloidal Hα intensity at the lower divertor exhibited no variation in baseline or peak amplitude, suggesting that ELM behavior was unaffected by the X-point displacement. In contrast, impurity signals in the core and edge showed distinct responses. As the X-point was shifted downward, the tungsten source signal from the lower divertor decreased significantly. Fig. 2(c) illustrates the corresponding strike point positions with different X-point positions; the W I signal was measured at the location marked with a blue cross. When the X-point was moved downward, the W I signal decreased even though the outer strike point approached the W I filterscope channel position. The mechanism underlying the observed reduction in tungsten source with X-point displacement is not yet clear and requires detailed transport analysis.

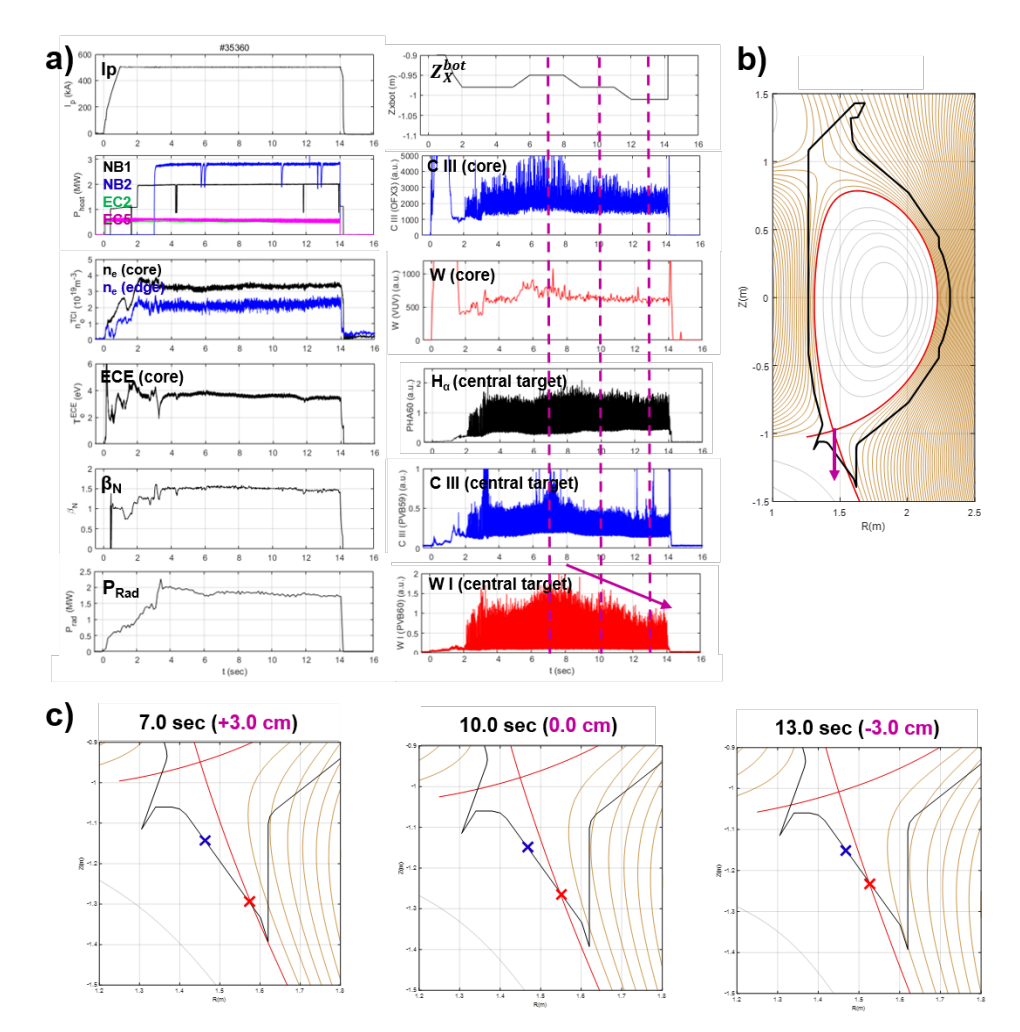


Fig. 2. a) The time evolution of plasma parameters of KSTAR discharge #35360. Left column: plasma current, heating power, core and edge electron density (two-color interferometer, TCI), core electron temperature, normalized beta, total radiated power and poloidal H_a intensity at lower divertor. Right column: Z coordinate of lower X-point, C III line at core (VSS), W line at core (VUV), poloidal H-alpha intensity, C III line (filterscope), W I line (filterscope) at central target of lower divertor. b) Magnetic flux at 10.0 sec. Magenta arrow show the direction of lower X-point movement. c) Lower divertor geometry (black line) and separatrix (red line) at 7.0 sec, 10.0 sec and 13.0 sec. Each time slice correspond to X-point height of +3.0 cm, 0.0 cm and -3.0 cm. Blue crosses denote the position of the visible filterscope channel for W I line (400.9 nm). Red crosses represent the positions of outer strike points

A similar scan was conducted in the upper single null (USN) configuration. Since only the lower divertor of KSTAR is composed of tungsten for now, it is difficult to know the upper plasma boundary effect on tungsten generation in LSN configuration. Therefore, in USN configuration, the height of lower X-point was scanned to vary the distance from lower plasma boundary to tungsten divertor target. Fig. 3 shows the time traces of plasma parameters of this experiment. Compared to previous experiment, the heating power was reduced significantly in an attempt to maintain the L-mode, but an H-mode plasma was created. As lower X-point moved down, the poloidal $H\alpha$ emission at ELM crash decreased significantly, while other plasma parameters did not changed distinctly.

At the reference equilibrium shape in Fig. 3(b), the lower X-point was located at $(R_X, Z_X) = (1.43 \text{ m}, -0.93 \text{ m})$. At 8.0 s, it was moved upward by +3.0 cm, returned to the reference position at 12.0 s, and moved downward by -3.0 cm at 16.0 s. As illustrated in the right column of Fig. 3(a), as lower X-point was shifted downward, both C III and W I intensities at the central divertor target decreased. The core tungsten emission also decreased, while the carbon emission in the core remained unchanged. However, further analysis is required to clarify the mechanisms responsible for the ELM mitigation and impurity source reduction. It is also worth noting that the W I intensity in the lower divertor under USN conditions was more than four times lower than in the LSN configuration.

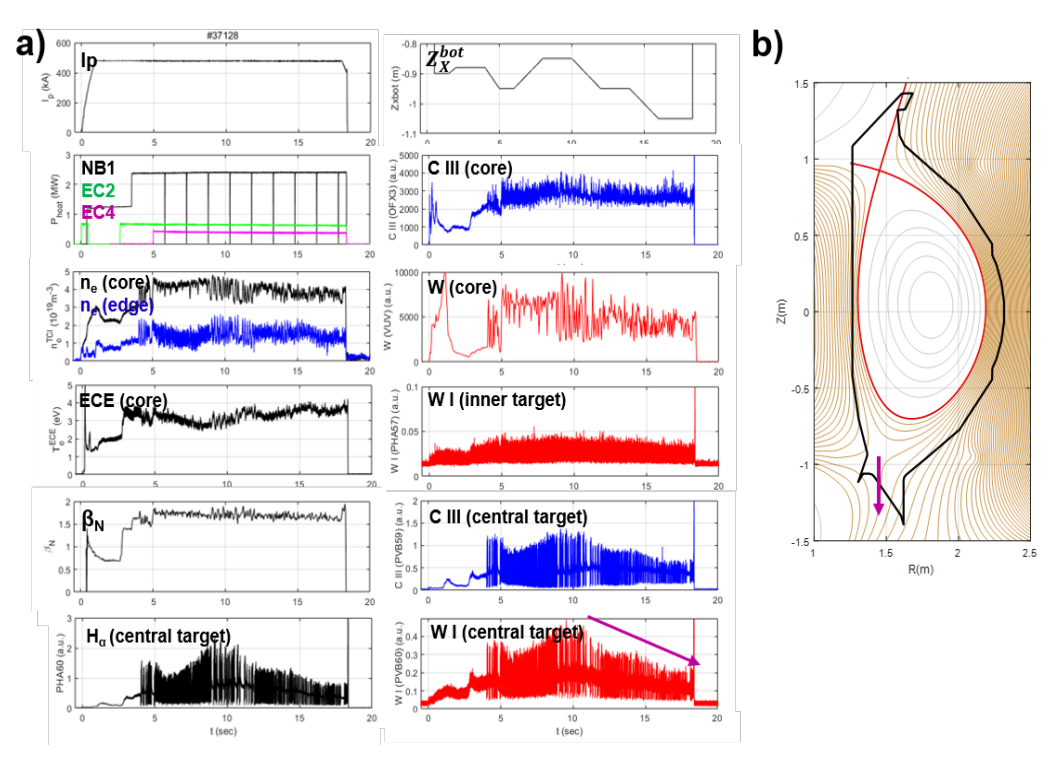


Fig.3. a) The time evolution of plasma parameters of KSTAR discharge #37128. Left column: plasma current, heating power, core and edge electron density (TCI), core electron temperature, normalized beta and poloidal Ha intensity at lower divertor. Right column: Z coordinate of lower X-point, C III line at core (VSS), W line at core (VUV), W I line at inner target of lower divertor (filerscope), C III line (filterscope), W I line (filterscope) at central target of lower divertor. b) Magnetic flux at 9.0 sec. Magenta arrow shows the direction of lower X-point movement

3.2. Tungsten source change with RMP

To mitigate tungsten source generation and core accumulation, experiments were also conducted using RMPs. Fig. 4 shows the plasma parameters for discharge #36872. An n=1 RMP field was applied at 4.0 s, with the in-vessel control coil (IVCC) current increased stepwise to achieve ELM mitigation. The IVCC current was ramped to 1 kA/t from 4.0 to 7.0 s, 2 kA/t from 9.0 to 12.0 s, and 2.5 kA/t thereafter. During the final phase, the plasma disrupted at 15.5 s due to mode locking. As the IVCC current increased, electron density, temperature, and normalized β decreased.

The poloidal $H\alpha$ intensity at the lower divertor confirmed that ELM activity was mitigated by the RMP. Visible filterscope measurement at lower divertor showed that both C III and W I line intensities decreased significantly once the RMP current reached 2 kA/t, whereas no change was observed at 1 kA/t. This behavior is consistent with the $H\alpha$ signal reduction. At the plasma core, VSS and VUV measurements showed that both C III and W line emissions decreased. These results suggest that ELM mitigation suppresses impurity source generation, which in turn reduces impurity accumulation in the core.

Previous studies from EAST have reported that RMP can directly affect impurity transport [8, 9]. In this study, RMPs applied in H-mode plasmas were found to affect both tungsten transport and source generation by ELMs. Follow-up experiments in L-mode plasma are planned to isolate the direct RMP effect on tungsten transport. In parallel, the unexpected reduction of carbon impurities—despite strike points being located above the tungsten divertor—will be further investigated. For a more quantitative assessment, tungsten influx at the divertor target will be evaluated using the S/XB method, while effective charge profiles will be reconstructed from visible bremsstrahlung measurements to estimate impurity content in the confined plasma. Complementary transport modeling will also be carried out to elucidate impurity production and transport mechanisms. In particular, the SOLEDGE3X code [10], developed by CEA–IRFM, will be employed. SOLEDGE3X provides a

fluid description of the edge plasma and is self-consistently coupled with EIRENE and ERO to account for plasma-neutral and plasma-wall interactions. By combining the 2D transport solver SOLEDGE2D with the 3D turbulence code TOKAM3X, SOLEDGE3X enables three-dimensional simulations of non-axisymmetric phenomena such as RMPs.

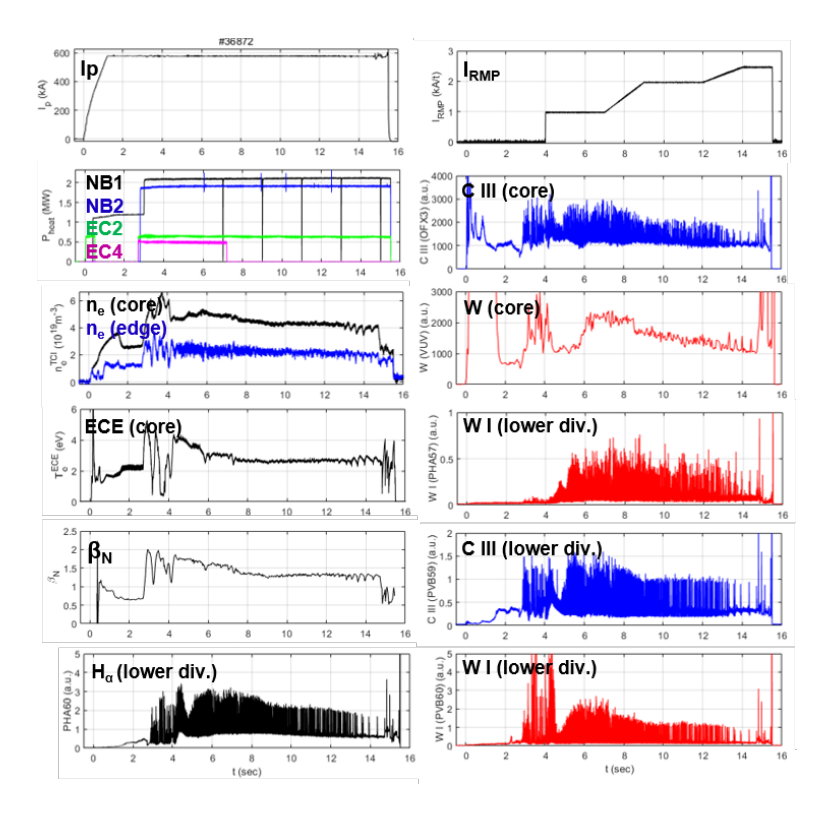


Fig. 4. The time evolution of plasma parameters of KSTAR discharge #36872. Left column: plasma current, heating power, core and edge electron density (TCI), core electron temperature, normalized beta and poloidal H-alpha intensity at lower divertor. Right column: IVCC current for RMP, C III line at core (VSS), W line at core (VUV), W I line at inner target of lower divertor (filerscope), C III line at central target of lower divertor (filterscope).

4. SUMMARY

Dedicated experiments in KSTAR with the tungsten divertor demonstrated that the tungsten source strongly depends on the plasma-target distance and ELM activity. In lower single null configuration, downward shift of the X-point led to a clear reduction of tungsten emission from divertor, despite global parameters remaining unchanged. Similarly, in upper single null configuration, the tungsten emission was reduced with downward shift of lower X-point while ELM behavior also changed. In addition, RMPs effectively mitigated ELMs and simultaneously reduced both tungsten and carbon impurity generation at the divertor, leading to decreased core accumulation. Future work will focus on quantitative source evaluation using the S/XB method, reconstruction of Zeff profiles, and transport modeling with SOLEDGE3X to establish predictive capability for KSTAR tungsten divertor.

ACKNOWLEDGEMENTS

This research was supported by the R&D Program "KSTAR Experimental Collaboration and Fusion Research (Grant No. EN2501-14)" through the Korea Institute of Fusion Energy (KFE), funded by the Government funds, Republic of Korea.

AUTHOR and OTHER-AUTHOR

[Left hand page running head is author's name in Times New Roman 8 point bold capitals, centred. For more than two authors, write **AUTHOR et al.**]

REFERENCES

- [1] Lee, H.H., et al., "Study on the tungsten source and transport during the first operation of the tungsten cassette monoblock divertor in the KSTAR tokamak", 3rd International Fusion and Plasma Conference, Seoul (2024)
- [2] Jang, J., et al., "Investigation of Behavior of Effective Charge (Zeff) in KSTAR plasmas", 3rd International Fusion and Plasma Conference, Seoul (2024)
- [3] Na, H.K., et al., "Configuration and installation design of optical diagnostic system on KSTAR", Fus. Eng. Des., 86 (2011)
- [4] Jang, J., et al., "Calibration of toroidal visible bremsstrahlung diagnostics and reconstruction of effective charge profiles in Korea Superconducting Tokamak Advanced Research (KSTAR)", Rev. Sci. Instrum. 95 (2024) 013503
- [5] Van Rooij G.J., et al., "Tungsten divertor erosion in all metal devices: Lessons from the ITER like wall of JET", J. Nucl. Mater. 438 (2013) S42
- [6] Seon, C.R. et al., "VUV spectroscopy in impurity injection experiments at KSTAR using prototype ITER VUV spectrometer", Rev. Sci. Instrum., 88 (2017) 083511
- [7] Song, I., et al., "Compact advanced extreme-ultraviolet imaging spectrometer for spatiotemporally varying tungsten spectra from fusion plasmas" Rev. Sci. Instrum., 88 (2017) 093509
- [8] Zhang, W., et al., "First observation of edge impurity behaviour with n=1 RMP application in EAST L-mode plasma", Nucl. Fusion 64 (2024) 086004
- [9] Dai, S.Y., et al., "EMC3-EIRENE modelling of tungsten behaviour under resonant magnetic perturbation on EAST: Effects of tungsten sputtering and impurity screening", Nucl. Fusion 63 (2020) 025003
- [10] Bufferand, H., et al., "Three-dimensional modelling of edge multi-component plasma taking into account realistic wall geometry", Nucl. Mater. Energy, 18 (2019) 82